# Asynchronous Reinforcement Learning Framework and Knowledge Transfer for Net-Order Exploration in Detailed Routing

Yibo Lin, *Member, IEEE*, Tong Qu, Zongqing Lu, Yajuan Su, and Yayi Wei

***Abstract*—The net orders in detailed routing are crucial to routing closure, especially in most modern routers following the sequential routing manner with the rip-up and reroute scheme. In advanced technology nodes, detailed routing has to deal with complicated design rules and large problem sizes, making its performance more sensitive to the order of nets to be routed. In the literature, the net orders are mostly determined by simple heuristic rules tuned for specific benchmarks. In this work, we propose an asynchronous reinforcement learning (RL) framework to automatically search for optimal ordering strategies and a transfer learning (TL) algorithm to improve performance. By asynchronous querying, the router, pretraining the RL agents, and finetuning with the TL algorithm, we can generate high-performance routing sequences to achieve a 26% reduction in the DRC violations and a 1.2% reduction in the total costs compared with the state-of-the-art detailed router.**

***Index Terms*—Detailed routing, physical design, policy distillation, reinforcement learning (RL), transfer learning (TL).**

## I. Introduction

ROUTING is a critical and time-consuming step in physical design [1]. Its solution impacts timing, power, and yield [2]. Routing is usually divided into global routing and detailed routing, with the former planning the rough routing regions and the latter finishing the actual interconnections [3]. Unlike global routing, detailed routing needs to handle plenty of design rules on a large grid graph. With feature sizes scaling down with the technology nodes, the routing grids become increasingly denser, leading to more complicated design rules from manufacturing, such as parallel-run spacing, end-of-line spacing, corner-to-corner spacing, and minimum area [4], [5]. Meanwhile, the grid graph for detailed routing is much larger than that of global routing, indicating larger solution space. As a result, detailed routing is becoming the most time-consuming step in advanced technology nodes [4].

While routing has been studied for several decades with many fundamental algorithms proposed, e.g., Lee's algorithm, A* search, negotiation-based rip-up and reroute (RRR) scheme, etc., most of the attention have been paid to global routing for a long time [3], [6], [7]. In the past few years, with advanced technology nodes coming to the stage, the importance of detailed routing has been realized. Various aspects of detailed routing have been investigated. For example, pin access issues have been discussed in [8]–[10]. Ahrens *et al.* explored specific data structures for efficient detailed routing [11]. Manufacturing constraints have also been explored in [12]–[14], such as lithography-friendly routing algorithms.

In recent ISPD contests [4], [5], detailed routing has been raised as a fundamental challenge in the backend design with practical benchmarks and realistic design rules. The contests largely stimulate the researches in detailed routing and several high-performance and robust routers have been proposed [15]–[19]. Sun *et al.* [20] proposed a valid pin access pattern generalization with a via-aware track assignment to minimize the overlaps between the wire segments. TritonRoute [15] adopted integer linear programming (ILP) for parallel intralayer routing. DRAPS [18] developed an A*-interval-based path search algorithm to handle complicated design rules. Dr. CU [16], [17], [21] proposed an optimal correct-by-construction path search algorithm and a two-level sparse data structure for runtime and memory efficiency. RDTA [19] developed an analytical approach to solve the track assignment problem following the global routing guides. Attention router explored reinforcement learning (RL) to solve the analog routing problem at a small scale [22].

Among the aforementioned detailed routers, most of them substantially follow the sequential routing strategy with the negotiation-based RRR scheme [16]–[18], [20]. The parallelism is usually obtained by routing a batch of nets far away enough from each other simultaneously. This means the routing order of nets is critical to the performance of the algorithm. Currently, the net ordering strategy is usually determined by simple heuristics. For instance, some net ordering indicators

Manuscript received 18 May 2021; revised 20 August 2021; accepted 23 September 2021. Date of publication 4 October 2021; date of current version 22 August 2022. This work was supported in part by the National Natural Science Foundation of China under Grant 61874002 and Grant 62034007; in part by Beijing Municipal Natural Science Foundation under Grant 2017ZX02315001; and in part by the National Key Research and Development Program of China under Grant 2019YFB2205005. The preliminary version has been presented at the Design, Automation and Test in Europe (DATE) Conference 2021. This article was recommended by Associate Editor L. Behjat. *(Corresponding authors: Yajuan Su; Yayi Wei.)*

Yibo Lin and Zongqing Lu are with the Computer Science Department, Peking University, Beijing 100871, China.

Tong Qu is with the Institute of Microelectronics, Chinese Academy of Sciences, Beijing 100029, China, and also with the School of Electronic, Electrical and Communication Engineering, University of Chinese Academy of Sciences, Beijing 100049, China.

Yajuan Su and Yayi Wei are with the Institute of Microelectronics, Chinese Academy of Sciences, Beijing 100029, China, also with the School of Microelectronics, University of Chinese Academy of Sciences, Beijing 100049, China, and also with Department of Computational Lithography, Guangdong Greater Bay Area Applied Research Institute of Integrated Circuit and Systems, Guangdong 510535, China (e-mail: suyajuan@ime.ac.cn; weiyayi@ime.ac.cn).

Digital Object Identifier 10.1109/TCAD.2021.3117505

are listed here: 1) the number of pins in a net; 2) the number of DRC violations caused by a net [23]; 3) the region size covered by a net [17]; and 4) the distance from a certain point [24]. In addition, the net order may change according to the current routing status and historical penalties during the RRR stage [3]. The performance of these ordering strategies may vary from design to design and from router to router as well. Therefore, a generic way to search for a good ordering strategy is desired to achieve high-performance routing.

To find a good ordering strategy, in this work, we formulate the strategy search problem into an RL task to automatically learn from the designs. The major contributions can be summarized as follows.

1) We develop an asynchronous RL framework to learn the ordering strategy in sequential detailed routing. By developing a customized neural network architecture, we can apply the learned model to different designs.
2) We propose a transfer learning (TL) algorithm that can adapt the pretrained policy to target designs by finetuning small, clipped regions for better performance.
3) The experimental results on ISPD 2018 and 2019 contest benchmarks [4], [5] demonstrate that the ordering strategy obtained from our framework generalizes well. Compared with the state-of-the-art detailed router Dr.CU 2.0 [17], the DRC violations and the total costs are reduced by 14 % and 0.7 %, respectively. With TL, we can reduce the DRC violations and the total costs by 26 % and 1.2 %, respectively.

The remainder of this article is organized as follows. Section II explains the background of routing, RL, TL, and problem formulation. Section III presents the RL framework details. Section IV explains the TL algorithm. Section V reports the experimental results on ISPD contest benchmarks. Finally, Section VI concludes this article.

## II. Preliminaries

In this section, we introduce the background on VLSI routing, RL, and problem formulation.

### A. Design Rules

More design rules are introduced in the advanced technology nodes. Meanwhile, three fundamental and representative design rules need to be considered [4].

1) *Short:* A via or wire segment of a net should not overlap with any object of another net.
2) *Spacing:* The spacing between two objects should satisfy the minimum distances. There are several different types of such requirements, e.g., end-of-line spacing, parallel-run spacing, and cut spacing.
3) *Minimum Area:* A metal polygon should have an area larger than the minimum threshold. Typical objectives for routing are to minimize the total wirelength and the DRC violations.

### B. Sequential Detailed Router

In year 2018 and 2019, the ISPD contest was organized on detailed routing [4], [5]. Dr.CU [17] won the first place in the

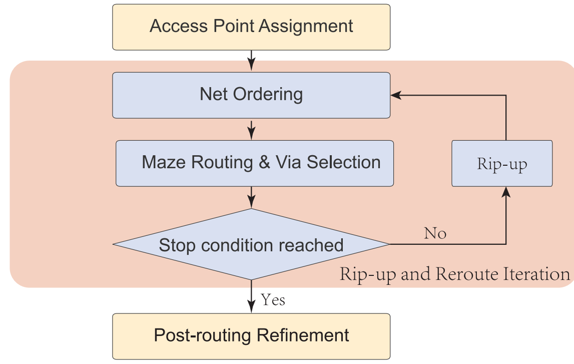


Fig. 1. Routing flow.

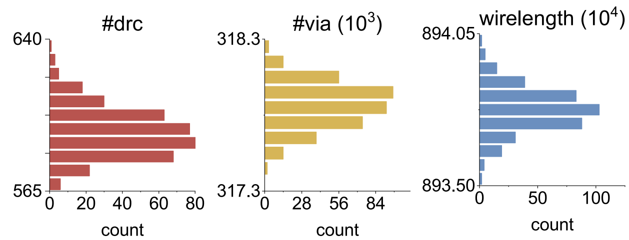


Fig. 2. Distribution of solution quality with random net ordering (300 iterations). The relative standard deviation of the number of DRC violations, the number of vias, and wirelength is 1.95 %, 0.04 %, and 0.008 %. Their ranges are 70.00, 845.00, and 4996.31, respectively.

ISPD 2019 contest and is open source. In this work, we adopt Dr.CU as the target detailed routing framework for studying, while the methodology can work on other routers as well. Fig. 1 illustrates its routing flow, which is a typical procedure for most sequential routing algorithms as well. Given a placed netlist, routing guides, routing tracks, and design rules, it first assigns access points for each pin. Then, it starts the RRR iterations to accomplish the routing. During the RRR iterations, if the router encounters congestion or DRC violations when trying to route a net, it rips up the net and the conflicted nets, leaving them for the next iteration to reroute. With enough iterations, the router can achieve convergence. Finally, it performs a postrouting refinement stage to reduce DRC violations. It needs to be noted that within each RRR iteration, Dr.CU also exploits parallelism between nets far away from each other, such that there will be no interaction when simultaneously solving the routing problem of each net. This does not change the sequential nature of the algorithm, i.e., routing in a net-by-net manner, as it does not determine the routing of different nets at the same time. The solution quality of sequential routers such as Dr.CU is highly correlated to the order of nets to be routed. Fig. 2 shows the distribution of solution quality with random net ordering routed by Dr.CU. Although the wirelength does not change much, the order affects both via count and the number of DRC violations. Thus, the ordering strategy needs to be carefully designed for high-quality routing across various benchmarks.

Dr.CU sorts nets by the routing region sizes (half-perimeter of the bounding box) of each net in descent order. In other words, nets covering large routing regions are routed first.

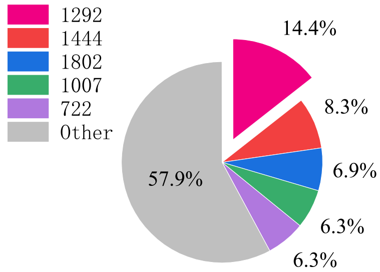


Fig. 3. Distribution of the net routing region sizes in `ispd18_test3`.

TABLE I
FEATURES OF EACH NET

| Feature | Dimension | Description |
|---|---|---|
| Size | 1 | The size of the routing region (half-perimeter of bounding box). |
| Degree | 1 | Number of nets with conflicts in its routing region. |
| Count | 1 | The number of times it has been routed/rerouted. |
| Cost | 1 | The weighted sum of violations on it. |
| Via | 1 | Number of via on it. |
| WL | 1 | Wirelength. |
| LA | 16 | Layer assignment. |

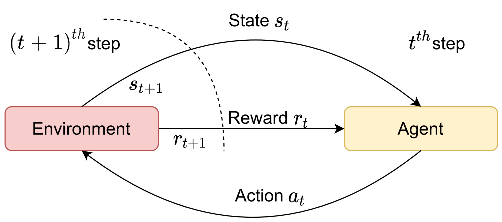


Fig. 4. Environment and agent system of RL.

However, we observe that the routing region sizes of different nets can be very similar, leading to random orders between these nets, and eventually causing high variations in the final violations. For example, Fig. 3 shows that 5293 nets have the same routing region size, accounting for 14.4% of the total number of nets in benchmark `ispd18_test3`. Therefore, there is a potential to improve the routing performance by developing an ordering strategy considering more features, which will be explained in detail in Section III-A and Table I.

### C. Reinforcement Learning

Machine learning (ML) is an effective practical tool to optimize a design in the absence of suitable models for optimization. One of the main obstacles in using supervised ML-based techniques for solving routing problems, especially the net ordering problems, is the lack of golden labeled datasets to learn. One way to overcome this problem is to use an RL approach. RL has been successfully applied in many applications. A typical RL problem can be considered as training an agent to interact with an environment. As illustrated in Fig. 4, at each step $t$, the agent $g$ observes a state $s_t \in \mathcal{S}$, takes an action $a_t \in \mathcal{A}$ based on $s_t$, receives a reward $r_t \in \mathcal{R}$, and then the state stochastically transits to the next state $s_{t+1}$. The objective is to learn a policy $\pi(a_t|s_t)$ that maximizes the expected cumulative reward $R = \sum_{i=0}^{\infty} \gamma^i r_{t+i}$, starting from any state $s$, where scalar $\gamma \in (0, 1]$ is a discount rate.

In this work, we define the environment as the router, and the design to be routed, the agent as a net-order planner that ranks the nets based on the features (state). The net ordering result is the action, and the reward is positively related to the solution quality, e.g., total wirelength and DRC violations.

### D. Problem Formulation

We define the net ordering problem in detailed routing as follows.

*Problem 1 (Net Ordering):* Given a set of nets $N$, train a net ordering policy that can generate a ranking score $s_i$ for each net $n_i \in N$ used by a sequential detailed router. The following metrics should be optimized simultaneously: 1) the total wirelength of all nets; 2) the number of the total used vias; and 3) the number of DRC violations.

We further define the TL problem to adapt the net ordering policy to a target design.

*Problem 2 (Transfer Learning):* Given a target design with a set of nets $N$ and a pretrained policy for net ordering, fine-tune the net ordering policy with small clipped regions of the target design. The performance metrics, as mentioned earlier, after routing the target design can be optimized.

## III. Reinforcement Learning Framework

In this section, we first define the state space, action space, reward, and the basic RL setup. Then, we explain the dedicated RL techniques for our routing problem.

### A. Basic RL Setup

We define the state space, action space, and reward as follows.

*State Space $\mathcal{S}$:* A state $s$ is the collective representation of features for all nets. Table I summarizes the seven features for each net. The first feature is the size of its routing region. The second feature is its degree, which denotes the number of nets whose routing region overlaps with it. The third feature is the number of times routed/rerouted so far. The remaining four features are its costs information, including the violations cost, wirelength, number of vias, and metal layers assignment.

*Action Space $\mathcal{A}$:* An action $a$ is a real number vector. Each number is defined as an ordering score of a net.

*Reward $\mathcal{R}$:* Given the ordering scores (action $a$), the environment (router) will provide its feedback (i.e., evaluation metrics). The agent receives a reward according to the environment's feedback. The reward $r$ is defined as

$$r = -c + c_o \tag{1}$$

where $c$ and $c_o$ are the total cost of all nets achieved by the agent's action $a$ and Dr.CU's default strategy. The total cost $c$ is defined as

$$c = \sum_{i=1}^{4} w_i x_i \tag{2}$$

where $x_i | i \in \{1, 2, 3, 4\}$ are the evaluation metrics used in the ISPD Contests, including short violation, spacing violation,

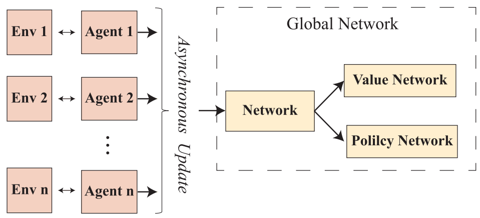


Fig. 5. A3C Framework with asynchronous parallel agents and global network.

number of vias, and wire length, and $w_i | i \in \{1, 2, 3, 4\}$ are the weights of the above metrics. The objective of the agent is to learn a policy to maximize the reward.

### *B. Asynchronous Advantage Actor–Critic Algorithm*

Expensive query to the environment is a typical challenge in RL, leading to slow convergence and unaffordable training time. We adopt an asynchronous advantage actor–critic (A3C) method [25] with multiple actor–critic (AC) agents running in parallel. This asynchronous RL framework can be defined as follows.

*Definition 1:* Given $m$ independent environments (designs), the corresponding $m$ agents are trained in parallel to get a policy $\pi$ that maximizes the rewards.

As shown in Fig. 5, each agent of A3C has a local copy of the policy and value networks. It performs actions in its environment to explore the solution space with a different policy. Different agents update the global network asynchronously during the training. A3C maintains a policy $\pi(a_t|s_t;\theta)$ and an estimate of the value function $V(s_t;\theta_v)$, where $\theta$ and $\theta_v$ are the global shared parameter vector.

Algorithm 1 illustrates how each actor is updated. After initialization, each agent takes a copy of the global shared network, with parameters $\theta'$ and $\theta'_v$ (line 5), and then runs the policy for $t_{\text{max}}$ steps or until a terminal state is reached. Finally, the agent computes the gradients in its process (lines 17 and 18) and then updates the global share network asynchronously.

### *C. Network Architecture*

We need two models in the A3C framework: 1) a policy network and 2) a value network. The policy network takes the state $s$ and outputs two arrays $(\mu, \sigma^2)$ that represent a normal distribution $\boldsymbol{p} \sim N(\mu, \sigma^2)$ over the actions. We pick the action by sampling from this normal distribution $\boldsymbol{p}$. We denote $\pi(a|s)$ as the probability of the sampled action $a$ given state $s$. The value network outputs the value function $V(s)$ (the expected return in rewards for state $s$ and action $a$), which is used to determine how advantageous it is in a particular state. Intuitively, the policy network tells us the ordering scores of the nets and the value network evaluates the scores in the sense of future rewards.

Fig. 6 plots the network architecture of the two models. We design the models in a special way so that the policy model can be used across different designs with different numbers of nets. To decouple the network architecture from the number

**Algorithm 1** Update Each A3C Actor [25]

**Require:** Global shared parameter vectors $\theta$, and $\theta_v$

1: Initialize thread step counter $t \leftarrow 1$
2: Define thread-specific copy of weights $\theta', \theta'_v$
3: **for** $T = 1, .., T_{max}$ **do**
4: $\quad d\theta \leftarrow 0$ and $d\theta_v \leftarrow 0$ ▷ Reset gradients
5: $\quad \theta' = \theta$ and $\theta'_v = \theta_v$
6: $\quad$ Get state $s_t$
7: $\quad t_{start} = t$
8: $\quad$ **repeat**
9: $\quad\quad$ Find action $a_t$ according to policy $\pi$
10: $\quad\quad$ Sort nets according action $a_t$
11: $\quad\quad$ Receive reward $r_t$ and new state $s_{t+1}$ from router
12: $\quad\quad t \leftarrow t + 1$
13: $\quad$ **until** terminal $s_t$ or $t - t_{\text{start}} == t_{\text{max}}$
14: $\quad$ Return $R = \begin{cases} 0 & \text{for terminal } s_t \\ V(s_t, \theta'_v) & \text{for non-terminal } s_t \end{cases}$
15: $\quad$ **for** $i = t - 1, \ldots, t_{start}$ **do**
16: $\quad\quad R \leftarrow r_i + \gamma R$
17: $\quad\quad d\theta \leftarrow d\theta + \nabla_{\theta'} \log \pi\left(a_i|s_i;\theta'\right)\left(R - V\left(s_i;\theta'_v\right)\right)$
18: $\quad\quad d\theta_v \leftarrow d\theta_v - \partial\left(R - V\left(s_i;\theta'_v\right)\right)^2 / \partial\theta'_v$
19: $\quad$ **end for**
20: $\quad$ Perform asynchronous update of $\theta$ using $d\theta$ and of $\theta_v$ using $d\theta_v$
21: **end for**

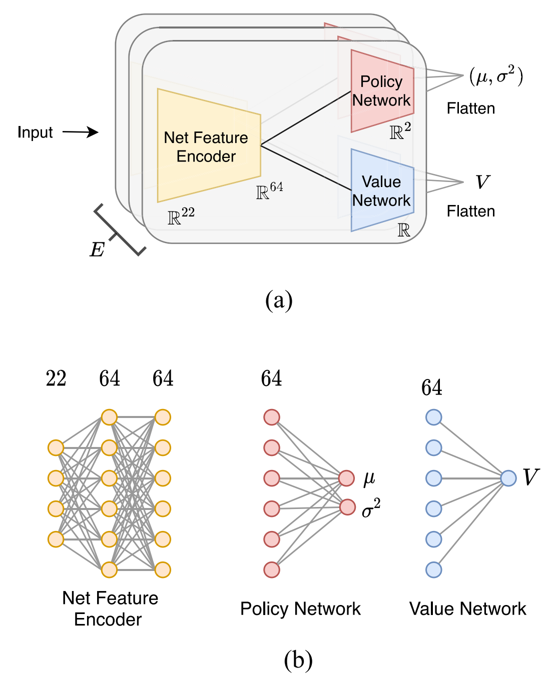


Fig. 6. Network structure. (a) Architecture of the policy and value networks, where $E$ denotes the number of nets. The net feature encoder encodes the features of each net. (b) Network Configuration.

of nets in design, we introduce a netwise feature encoding network that encodes the features of each net independently. We then concatenate the encoded features for the policy and value networks. For example, given a design with $E$ nets, the encoder will encode the $\mathbb{R}^{E\times 22}$ input feature tensor into an $\mathbb{R}^{E\times 64}$ tensor. The policy network takes this tensor and generates an array of ordering scores for all nets, i.e., $\mathbb{R}^{E\times 2}$ (mean and variance of the probability distribution for each net). We then sample from a normal distribution for each net to get its ordering score. In our implementation, $\mu$ is modeled by a linear layer and $\sigma^2$ by a softplus layer. The value network flattens the feature tensor and feeds into a fully connected layer with $E \times 64$ hidden units to obtain a scalar at the output.

The major benefit of such a network architecture is that the policy network can be shared across different designs, as we essentially perform netwise modeling with the ordering score of each net dependent on its features only. While it is true that using a more complicated model that correlates the features of multiple nets may help to explore better policy, current architecture still has enough expressive power to verify the main idea of using RL in solving the net ordering problem. We leave the exploration of complicated models in the future. For example, we can determine the ranking score of a net by multiple related nets. This requires the model to be able to learn the correlation of features between multiple nets.

### D. Mismatch Penalty

General RL framework initializes the neural networks in a random manner, which may cause slow convergence in our problem, especially when obtaining the reward from the environment (i.e., running the router) is very time consuming. On the other hand, we do have the prior knowledge to this problem that the default ordering strategy of using routing region sizes in Dr.CU is a generally good policy compared with a random one. Incorporating such knowledge has the potential to speed up training. Hence, (1) is modified to

$$r = -c + c_o - \frac{\alpha}{k}\sum_{i=1}^{k} \Delta {a_i}^2 \qquad (3)$$

where $\Delta a$ is the difference between the predicted ordering scores and the sizes of routing regions, $\alpha$ is a user-defined parameter, and $k$ is the number of nets to be routed. The parameter $\alpha$ is positive only at the early training steps and then set to zero. The detailed setup can be found in Section V. Fig. 7 compares the learning speeds of the two reward function defining methods. The results show that the method of adding a mismatch penalty tends to learn faster. As we only apply the mismatch penalty at the early stage of the training, it will speed up the training, but not limit the exploration space to the heuristic ordering strategy used in Dr.CU. In other words, the agent is free to generate different orders from that in Dr.CU.

## IV. Transfer Learning Algorithm

In this section, we first introduce the TL algorithm based on policy distillation. In the end, we summarize the overall flow of our TL algorithm.

We assume a reasonably good policy is available. Our task is to mine the knowledge from the pretrained policy and adapt to a target design to improve the performance.

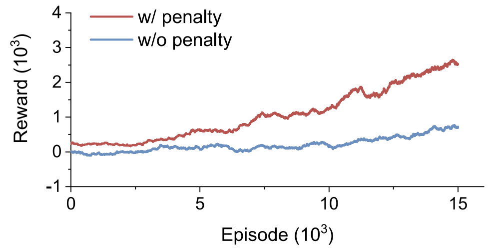


Fig. 7. Comparison of two reward functions. The curves represent the moving average reward of the last 1000 episodes (one episode includes four RRR iterations according to the setting of Dr.CU). We train the agents for 15 000 episodes and the maximum training time is within 24 h. Mismatch penalty enables faster reward increase.

### A. Policy Distillation Algorithm

In the previous section, we aim at training a general RL policy to solve the net ordering tasks of multiple designs, which is essentially a multitask learning problem. However, it is not always easy to achieve good generality across a wide range of designs. On designs with unique characteristics, a generally good policy may not capture the unique design styles and eventually fails to result in high solution quality. If we can customize the policy for each design with low overhead, there is an opportunity to improve the performance further. To reduce the overhead of customization, we fine-tune the well-trained policy from the previous section using a small region clipped from the target design instead of training from scratch. In this way, we can minimize the TL overhead by repeatedly routing the target design when the agents interact with the environment. The key for TL is to effectively transfer the knowledge from the source domain (i.e., the pretrained policy) to the target domain (i.e., for routing the target design).

*Policy distillation* is a TL approach that distills the knowledge from a teacher network to a student network. Typical RL policy distillation frameworks transfer the teacher policy in a supervised learning paradigm. Specifically, a student policy is learned by minimizing the Kullback–Leibler (KL) divergence of actions between the teacher policy $\pi^S$ and student policy $\pi^T$ [26]. As explained in Section III-C, one action $a$ is sampled from the normal distribution $\boldsymbol{p}$ from the policy network, so the policy distillation can be completed by optimizing the per-time-step KL divergence between the distributions of the teacher and the student over actions

$$L_{\mathrm{KL}}\left(D, \theta^S\right) = \sum_{t=1} \boldsymbol{p}_t^T \log \frac{\boldsymbol{p}_t^T}{\boldsymbol{p}_t^S} \qquad (4)$$

where $\boldsymbol{p}_t^T$ is the normal distribution from the teacher network at step $t$, $\boldsymbol{p}_t^S$ is the distribution from the student network of this step, $\theta^S$ denotes the parameters of the student policy network, and $D$ is a set of distributions from the teacher network.

### B. Policy Transfer Flow

As our network structure in Section III-C is decoupled with the number of nets, different designs' action spaces can be considered as the same dimensions. Hence, the student network can directly mimic the action pattern of the teacher network.

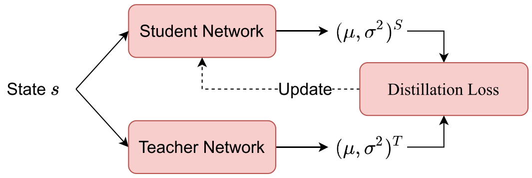


Fig. 8. Distillation procedure.

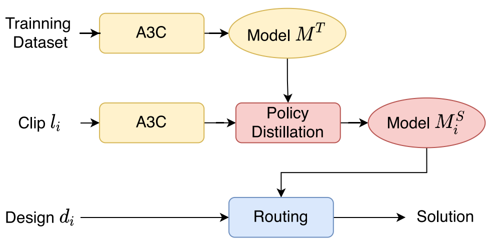


Fig. 9. Overall flow.

Based on the above observation, we propose a policy distillation flow to transfer knowledge between designs. As illustrated in Fig. 8, the distribution $\boldsymbol{p}$ of the teacher network from a source design (environment) $E^T$ is used as our supervision to update the student network of target design (environment) $E^S$. This procedure is performed by minimizing (4) over student policy network parameters $\theta^S$ for $E^S$ and $\theta^S$, including the net feature encoder, value layer, and policy layer. The input to both the teacher and the student networks is the state $s$ of environment $E^S$. It means that we want to transfer the expertise from the environment $E^T$ toward the current state. Symbol $D$ is a set of distributions from the teacher network in one batch.

Suppose we have already had a reasonably good policy for most designs. We want to use the knowledge from the policy to improve the performance of a particular design further. In the proposed TL approach, we first select a clip from the target design because training on a complete design is not affordable, mainly when the design contains tens of thousands of nets. Given a representative clip, we observe that training can significantly reduce the training time without much performance loss. Then, we train the student network by interacting with the clip (environment) $E^S$ for a certain amount of steps, e.g., 1000 steps in the experiments. Afterward, we start performing policy distillation.

### C. Overall Flow

Fig. 9 shows the overall flow. The A3C algorithm is first used to train on multiple designs to obtain the pretrained model $M^T$. For each input design $d_i$ to be routed, we select a clip $l_i$ from it. The policy distillation is performed to guide the model $M_i^S$, which is trained on the clip $l_i$. After a certain period of training, the best model for clip $l_i$ is selected. Finally, the input design $d_i$ is routed under the guidance of model $M_i^S$.

The overall routing flow is summarized in Algorithm 2, given that the RL model $M_i^S$ is to determine the net ordering. We first extract features for each net to be routed within each routing iteration and then obtain the ordering scores using

**Algorithm 2** Overall Routing Flow Using RL Model

**Require:** A set of nets $N$ in design $t_i$, RL model $M_i^S$, and various design rules for a router
**Ensure:** Routing solution with optimized solution quality
1: Define $M$ as the maximum number of iterations of RRR.
2: Define $S$ as the set of nets' ordering scores.
3: $i \leftarrow 0$
4: **while** $i < M, N \neq \emptyset$ **do**
5: $\quad i \leftarrow i + 1$
6: $\quad$ **for all** net $n \in N$ **do**
7: $\quad\quad$ Extract net features $f_n$
8: $\quad$ **end for**
9: $\quad$ Use the RL policy $\pi$ and features $F$ to get the ordering scores of all nets $S$
10: $\quad$ batch list $B = \textbf{Scheduler}(N, S)$
11: $\quad$ **for all** $b \in B$ **do**
12: $\quad\quad$ Run maze routing, via selection and post-routing in multiple threads
13: $\quad$ **end for**
14: $\quad$ Calculate the total cost
15: $\quad$ **for all** $n \in N$ **do**
16: $\quad\quad$ **if** $n$ meet constraints **then**
17: $\quad\quad\quad$ Pop $n$ from $N$
18: $\quad\quad$ **else**
19: $\quad\quad\quad$ Rip-up $n$
20: $\quad\quad$ **end if**
21: $\quad$ **end for**
22: **end while**

the RL policy (line 9). After that, we leverage Dr.CU to finish each RRR iteration (lines 10–19). More specifically, we schedule all batches at the beginning of an RRR iteration (line 10) by sorting the nets according to the scores and dividing them into batches. Nets within a batch that do not conflict with each other can be routed parallel to reduce the runtime [16]. If the RRR stopping criteria are not met, the iterations will continue until the maximum number of iterations is reached. We keep the same settings as Dr.CU except for the net ordering.

## V. Experimental Results

### A. Experimental Setup

We define our environment using the OpenAI Gym interface with Dr.CU 2.0 [17] as the detailed router, and implement our RL agent network in PyTorch. All the experiments ran on a 64-bit Linux machine with two 20-core Intel Xeon@2.1 -GHz CPUs and 64 -GB RAM.

The latest design benchmarks available to academics are the ISPD 2018 and ISPD 2019 initial detailed routing contests [4], [5] benchmarks, which have 20 designs. We experiment on those benchmarks. The detailed information of the benchmarks is shown in Table II. We can see that benchmarks have quite different problem sizes and technology nodes (32/45/65 nm).

As the benchmarks are large, we select clips with suitable scales and add them to the training dataset. The procedure

TABLE II
CHARACTERISTICS OF ISPD 2018 AND 2019 CONTEST BENCHMARKS

| | benchmarks | #std | #net | Die size ($mm^2$) | Tech. node (nm) |
|---|---|---|---|---|---|
| ISPD18 | test1 | 8879 | 3153 | $0.20 \times 0.19$ | 45 |
| | test2 | 35 913 | 36 834 | $0.65 \times 0.57$ | 45 |
| | test3 | 35 973 | 36 700 | $0.99 \times 0.70$ | 45 |
| | test4 | 72 094 | 72 401 | $0.89 \times 0.61$ | 32 |
| | test5 | 71 954 | 72 394 | $0.93 \times 0.92$ | 32 |
| | test6 | 107 919 | 107 701 | $0.86 \times 0.53$ | 32 |
| | test7 | 179 865 | 179 863 | $1.36 \times 1.33$ | 32 |
| | test8 | 191 987 | 179 863 | $1.36 \times 1.33$ | 32 |
| | test9 | 192 911 | 178 857 | $0.91 \times 0.78$ | 32 |
| | test10 | 290 386 | 182 000 | $0.91 \times 0.87$ | 32 |
| ISPD19 | test1 | 8879 | 3153 | $0.148 \times 0.146$ | 32 |
| | test2 | 72 094 | 72 410 | $0.873 \times 0.589$ | 32 |
| | test3 | 8283 | 8953 | $0.195 \times 0.195$ | 32 |
| | test4 | 146 442 | 151 612 | $1.604 \times 1.554$ | 65 |
| | test5 | 28 920 | 29 416 | $0.906 \times 0.906$ | 65 |
| | test6 | 179 881 | 179 863 | $1.358 \times 1.325$ | 32 |
| | test7 | 359 746 | 358 720 | $1.581 \times 1.517$ | 32 |
| | test8 | 539 611 | 537 577 | $1.803 \times 1.708$ | 32 |
| | test9 | 899 341 | 895 253 | $2.006 \times 2.151$ | 32 |
| | test10 | 899 404 | 895 253 | $2.006 \times 2.151$ | 32 |

**Algorithm 3** Clip Selection

1: Define $H_C$ and $W_C$ as the initial width and height of a clip $C$, and $N_C$ as the step size.
2: **while** the number of nets in clip $C$ is smaller than 500 **do**
3: Divide the benchmarks into clips with sizes of $H_C \times W_C$
4: Choose the clip with the highest pin density as the candidate clip $C$
5: Project pins outside the clip $C$ to the boundary
6: $W_C \leftarrow W_C + N_C$
7: $H_C \leftarrow H_C + N_C$
8: **end while**
9: Add the clip $C$ into the training dataset

of clip selection is described in Algorithm 3. The idea is to select a dense clip including around 500 nets because we observe this is an affordable scale to invoke the router during training repeatedly. We first divide a benchmark into fixed-size clips (line 3) and then choose the densest one in terms of pins (line 4). We then project the pins outside the clip to its boundary (line 5). If the number of nets in the clip exceeds 500, we add it to the training dataset. Otherwise, we expand the clip to include more nets and repeat the above steps.

### *B. Asynchronous Advantage Actor–Critic*

In this section, we verify the effectiveness of the A3C framework. We set the discount factor $\gamma = 0.99$, the coefficient for the value loss $\beta = 0.25$, entropy cost $\eta = 0.001$, and learning rate to 0.001. We also set $\alpha = 0.1$ for the first 100 training episodes and reduce to 0 afterward. A standard noncentered RMSProp is used as the gradient ascent optimizer. The neural network weights are initialized randomly. We use eight AC agents to train in parallel, and the maximum training time is set to 24 h (around 8000 episodes).

According to Dr.CU [17], the runtime of routing one of these benchmarks varies from 2 min to 5 h. Ideally, it is expected to train and test an RL model on one technology node only. However, considering that most designs in Table II are in the 32-nm node, while the ones in 45-/65 -nm nodes are either too small or large, we choose a training dataset mixed with designs in 32- and 45-nm nodes, and test on the remaining to validate the framework. To balance the runtime overhead and universality of the generated model, `ISPD18_test3/5/6/7` are selected as benchmarks in the training dataset and the remaining sixteen as the test dataset. Due to `ISPD18_test7`'s large size, we choose two clips from it containing 7 and 26 violations to put in the training dataset. In conclusion, the training dataset contains {two regions clipped from `ISPD18_test7`, `ISPD18_test3/5/6`}. These training benchmarks have moderate and diverse sizes that can keep reasonable training time but also complicated enough to represent the real routing challenges.

Tables III and IV summarize the results of the training and testing datasets. We compare the wirelength, number of vias, DRC violations, total cost, and runtime between our RL framework and Dr.CU [17]. The violation values here are a summation of all the DRC violations mentioned in (1). In the training dataset, with similar wirelength and number of vias, we can achieve 13% fewer DRC violations compared with the default policy in Dr.CU. The total cost only has small improvements. This is because the cost is dominated by wirelength due to its large scale according to its definition in the contests. The results on the training dataset indicate that our RL framework and training techniques are able to learn good policies from the benchmarks. We also observe around 6 % runtime overhead, which mostly comes from the feature extraction and the system integration between the `Python`-based RL agent and the `C++`-based Dr.CU implementation. In the testing dataset, our policy can achieve an average of 14 % improvement in violations and 0.7 % in total cost without degradation in wirelength and number of vias. The results on the testing dataset demonstrate that the policy learned from the training dataset can generalize to unseen benchmarks and achieve high-quality solutions on average.

One needs to be mentioned that on large benchmarks such as `ISPD19_test7-10` in 32-nm technology node, the RL policy can reduce the violations by 40 %–50 %, which is rather promising. However, we observe that there are also outliers, such as `ISPD18_test4` and `ISPD19_test4`, where the violations increase by 15 % and 46 %, respectively. The results of all the remaining benchmarks are either improved or within a comparable range. We speculate that the two outliers contain special features not in our training dataset or state space, causing unusual behaviors. `ISPD19_test4` is in 65-nm technology node with six metal layers, while the designs in the training dataset are in 45-/32-nm technology nodes with nine metal layers. These differences probably reduce the generalization performance of the RL policy in these two designs. At this point, we have obtained a model that can perform well in most design, and further improvement will be completed in TL.

TABLE III
EXPERIMENTAL RESULTS ON THE TRAINING DATASET (COMPARISON BETWEEN DR.CU [17] AND RL [27])

| | | Absolute Values | | | | | | | | | |
|---|---|---|---|---|---|---|---|---|---|---|---|
| | | Wirelength ($10^7$) | | #via ($10^6$) | | #vio | | Cost ($10^7$) | | T (s) | |
| | Design | Dr.CU | RL | Dr.CU | RL | Dr.CU | RL | Dr.CU | RL | Dr.CU | RL |
| ISPD18 | test3 | 0.894 | 0.894 | 0.318 | 0.318 | 361 | 342 | 0.529 | 0.528 | 172 | 189 |
| | test5 | 2.870 | 2.870 | 0.966 | 0.965 | 393 | 388 | 1.648 | 1.648 | 610 | 638 |
| | test6 | 3.700 | 3.701 | 1.481 | 1.481 | 95 | 63 | 2.151 | 2.150 | 756 | 793 |
| | test7 | 6.727 | 6.728 | 2.403 | 2.403 | 792 | 735 | 3.884 | 3.881 | 1466 | 1576 |
| | | Relative Ratios | | | | | | | | | |
| | | Wirelength | | #via | | #vio | | Cost | | T | |
| | Design | Dr.CU | RL | Dr.CU | RL | Dr.CU | RL | Dr.CU | RL | Dr.CU | RL |
| ISPD18 | test3 | 1.000 | 1.000 | 1.000 | 1.000 | 1.000 | 0.947 | 1.000 | 0.998 | 1.000 | 1.099 |
| | test5 | 1.000 | 1.000 | 1.000 | 0.999 | 1.000 | 0.987 | 1.000 | 1.000 | 1.000 | 1.046 |
| | test6 | 1.000 | 1.000 | 1.000 | 1.000 | 1.000 | 0.663 | 1.000 | 1.000 | 1.000 | 1.049 |
| | test7 | 1.000 | 1.000 | 1.000 | 1.000 | 1.000 | 0.928 | 1.000 | 0.999 | 1.000 | 1.075 |
| | Min. | 1.000 | 1.000 | 1.000 | 0.999 | 1.000 | 0.663 | 1.000 | 0.998 | 1.000 | 1.046 |
| | Max. | 1.000 | 1.000 | 1.000 | 1.000 | 1.000 | 0.987 | 1.000 | 1.000 | 1.000 | 1.099 |
| | Geo. Mean | 1.000 | 1.000 | 1.000 | 1.000 | 1.000 | 0.870 | 1.000 | 0.999 | 1.000 | 1.067 |

### C. Transfer Learning via Policy Distillation

In this section, we design experiments to illustrate the effectiveness of the policy distillation algorithm. We obtained a generally good model in previous experiments, but there are some outliers, such as `ISPD18_test4` and `ISPD19_test4`. This result indicates that the knowledge gained in the training dataset has insufficient generalization capabilities. Therefore, we transfer the knowledge from the pretrained policy to the student network for each design via policy distillation. One challenge is that the routing of each design is time consuming in the testing dataset. As we mentioned before, for each design $d_i$ to be tested, we select a clip $l_i$ from it for interaction. The clip $l_i$ must have sufficient representation. We select a clip containing about 500 nets from the region with the highest pin density such that the routing can be finished within 1 min by Dr.CU. Pin density is a straightforward metric for clip selection. We leave the exploration of more complicated clipping strategies to the future. In the following experiments, we maintain consistent hyperparameters of the network structures across all designs.

The student agents are trained with the clip $l_i$ only and perform policy distillation after 1000 episodes. We set the maximum time for the entire training to 3 h (assume the maximum time available for TL is equivalently around 3000 episodes). Finally, the model is evaluated with the design $d_i$. Table IV shows the comparison of wirelength, number of vias, number of DRC violations, and total costs between Dr.CU, the RL algorithm [27], and the TL algorithm. By enabling TL, we can further reduce the average number of DRC violations by 12% and the average total cost by 0.5% compared with the RL algorithm, while other metrics remain almost the same as the RL algorithm. Note that these numbers are an extra improvement from the RL algorithm. Compared with Dr.CU, the TL algorithm can contribute to 26% reduction of DRC violations and 1.2% reduction of total cost.

To further verify the performance of the model with additional training iterations, we also train the model for 100 K episodes on `ISPD19_test2` and `ISPD19_test8`, and show the training curves in Fig. 10. As routing an entire design to obtain the number of DRC violations is time consuming, we only sample every 1000 and 4000 episodes for these designs, respectively. We can see that the performance of the TL curves continues to improve and gradually saturates at 60 K–100 K episodes. We also plot the curves of training from scratch using the RL algorithm as "RL-S" in the figure. Compared

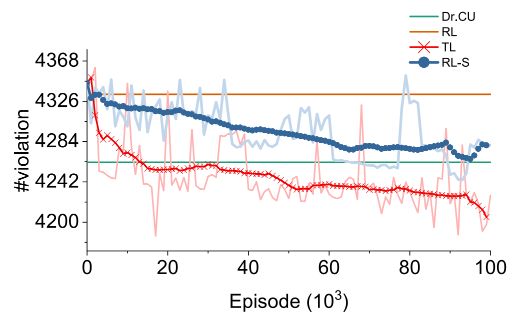


(a)

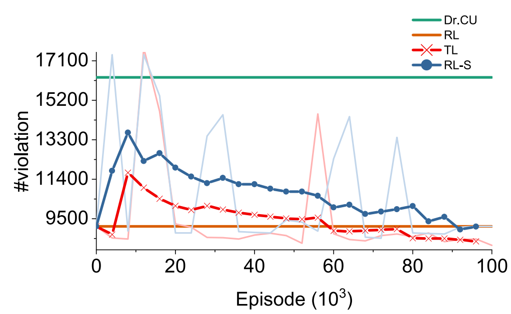


(b)

Fig. 10. Performance with additional training iterations on `ISPD19_test2` and `ISPD19_test8`. The raw TL/RL-S results are shown in light red/blue, and the average TL/RL-S results are shown in the blue/green by taking an average of 25 data points around each point. (a) `ISPD19_test2`. (b) `ISPD19_test8`.

TABLE IV
EXPERIMENTAL RESULTS ON THE TESTING DATASET (COMPARISON BETWEEN DR.CU [17], RL [27], AND TL)

**Absolute Values**

| | | Wirelength ($10^7$) | | | #via ($10^6$) | | | #vio | | | Cost ($10^7$) | | | T (s) | | |
|---|---|---|---|---|---|---|---|---|---|---|---|---|---|---|---|---|
| | Design | Dr.CU | RL | TL | Dr.CU | RL | TL | Dr.CU | RL | TL | Dr.CU | RL | TL | Dr.CU | RL | TL |
| ISPD18 | test1 | 0.05 | 0.05 | 0.05 | 0.03 | 0.03 | 0.03 | 1 | 0 | 0 | 0.03 | 0.03 | 0.03 | 9 | 10 | 10 |
| | test2 | 0.81 | 0.81 | 0.81 | 0.33 | 0.33 | 0.33 | 1 | 4 | 4 | 0.47 | 0.47 | 0.47 | 125 | 136 | 137 |
| | test4 | 2.70 | 2.70 | 2.70 | 0.73 | 0.73 | 0.73 | 507 | 584 | 487 | 1.52 | 1.52 | 1.52 | 696 | 745 | 727 |
| | test8 | 6.76 | 6.76 | 6.76 | 2.41 | 2.41 | 2.41 | 819 | 756 | 753 | 3.90 | 3.90 | 3.90 | 1474 | 1541 | 1548 |
| | test9 | 5.69 | 5.69 | 5.69 | 2.41 | 2.41 | 2.41 | 139 | 54 | 9 | 3.33 | 3.33 | 3.33 | 1196 | 1260 | 1240 |
| | test10 | 7.04 | 7.04 | 7.04 | 2.59 | 2.59 | 2.60 | 8271 | 9165 | 8915 | 4.45 | 4.50 | 4.49 | 2244 | 2373 | 2315 |
| ISPD19 | test1 | 0.07 | 0.07 | 0.07 | 0.04 | 0.04 | 0.04 | 1121 | 1110 | 1045 | 0.10 | 0.10 | 0.09 | 102 | 109 | 106 |
| | test2 | 2.56 | 2.56 | 2.56 | 0.79 | 0.79 | 0.79 | 4262 | 4333 | 4253 | 1.65 | 1.66 | 1.65 | 1499 | 1610 | 1625 |
| | test3 | 0.09 | 0.09 | 0.09 | 0.06 | 0.07 | 0.07 | 167 | 96 | 77 | 0.07 | 0.06 | 0.06 | 52 | 54 | 54 |
| | test4 | 3.13 | 3.13 | 3.13 | 1.03 | 1.03 | 1.03 | 5455 | 7968 | 7949 | 2.04 | 2.17 | 2.17 | 1548 | 1653 | 1665 |
| | test5 | 0.49 | 0.49 | 0.49 | 0.15 | 0.15 | 0.15 | 408 | 426 | 436 | 0.30 | 0.30 | 0.30 | 154 | 163 | 165 |
| | test6 | 6.78 | 6.78 | 6.78 | 1.99 | 1.99 | 1.98 | 8944 | 9474 | 9363 | 4.23 | 4.26 | 4.25 | 3158 | 3340 | 3374 |
| | test7 | 12.72 | 12.72 | 12.71 | 4.81 | 4.81 | 4.80 | 11649 | 7798 | 7577 | 7.90 | 7.71 | 7.69 | 7812 | 8338 | 8379 |
| | test8 | 19.56 | 19.56 | 19.55 | 7.33 | 7.33 | 7.32 | 16291 | 9128 | 8676 | 12.06 | 11.70 | 11.67 | 11089 | 11870 | 11855 |
| | test9 | 29.73 | 29.73 | 29.72 | 12.19 | 12.20 | 12.17 | 34632 | 16745 | 16015 | 19.03 | 18.14 | 18.10 | 15225 | 15967 | 15681 |
| | test10 | 29.46 | 29.45 | 29.45 | 12.48 | 12.49 | 12.49 | 32743 | 18150 | 17522 | 18.86 | 18.13 | 18.10 | 16156 | 17108 | 17335 |

**Relative Ratios**

| | | Wirelength | | | #via | | | #vio | | | Cost | | | T | | |
|---|---|---|---|---|---|---|---|---|---|---|---|---|---|---|---|---|
| | Design | Dr.CU | RL | TL | Dr.CU | RL | TL | Dr.CU | RL | TL | Dr.CU | RL | TL | Dr.CU | RL | TL |
| ISPD18 | test1 | 1.000 | 1.000 | 1.000 | 1.000 | 1.000 | 1.000 | 1.000 | 0.000 | 0.000 | 1.000 | 1.000 | 1.000 | 1.000 | 1.111 | 1.111 |
| | test2 | 1.000 | 1.000 | 1.000 | 1.000 | 1.000 | 1.000 | 1.000 | 4.000 | 4.000 | 1.000 | 1.000 | 1.000 | 1.000 | 1.088 | 1.096 |
| | test4 | 1.000 | 1.000 | 1.000 | 1.000 | 1.000 | 1.000 | 1.000 | 1.152 | 0.961 | 1.000 | 1.000 | 1.000 | 1.000 | 1.070 | 1.045 |
| | test8 | 1.000 | 1.000 | 1.000 | 1.000 | 1.000 | 1.000 | 1.000 | 0.923 | 0.919 | 1.000 | 1.000 | 1.000 | 1.000 | 1.045 | 1.050 |
| | test9 | 1.000 | 1.000 | 1.000 | 1.000 | 1.000 | 1.000 | 1.000 | 0.388 | 0.065 | 1.000 | 1.000 | 1.000 | 1.000 | 1.054 | 1.037 |
| | test10 | 1.000 | 1.000 | 1.000 | 1.000 | 1.000 | 1.004 | 1.000 | 1.108 | 1.078 | 1.000 | 1.011 | 1.009 | 1.000 | 1.057 | 1.032 |
| ISPD19 | test1 | 1.000 | 1.000 | 1.000 | 1.000 | 1.000 | 1.000 | 1.000 | 0.990 | 0.932 | 1.000 | 1.000 | 0.900 | 1.000 | 1.069 | 1.039 |
| | test2 | 1.000 | 1.000 | 1.000 | 1.000 | 1.000 | 1.000 | 1.000 | 1.017 | 0.998 | 1.000 | 1.006 | 1.000 | 1.000 | 1.074 | 1.084 |
| | test3 | 1.000 | 1.000 | 1.000 | 1.000 | 1.167 | 1.167 | 1.000 | 0.575 | 0.461 | 1.000 | 0.857 | 0.857 | 1.000 | 1.038 | 1.038 |
| | test4 | 1.000 | 1.000 | 1.000 | 1.000 | 1.000 | 1.000 | 1.000 | 1.461 | 1.457 | 1.000 | 1.064 | 1.064 | 1.000 | 1.068 | 1.076 |
| | test5 | 1.000 | 1.000 | 1.000 | 1.000 | 1.000 | 1.000 | 1.000 | 1.044 | 1.069 | 1.000 | 1.000 | 1.000 | 1.000 | 1.058 | 1.071 |
| | test6 | 1.000 | 1.000 | 1.000 | 1.000 | 1.000 | 0.995 | 1.000 | 1.059 | 1.047 | 1.000 | 1.007 | 1.005 | 1.000 | 1.058 | 1.068 |
| | test7 | 1.000 | 1.000 | 0.999 | 1.000 | 1.000 | 0.998 | 1.000 | 0.669 | 0.650 | 1.000 | 0.976 | 0.973 | 1.000 | 1.067 | 1.073 |
| | test8 | 1.000 | 1.000 | 0.999 | 1.000 | 1.000 | 0.999 | 1.000 | 0.560 | 0.533 | 1.000 | 0.970 | 0.968 | 1.000 | 1.070 | 1.069 |
| | test9 | 1.000 | 1.000 | 1.000 | 1.000 | 1.001 | 0.998 | 1.000 | 0.484 | 0.462 | 1.000 | 0.953 | 0.951 | 1.000 | 1.049 | 1.030 |
| | test10 | 1.000 | 1.000 | 1.000 | 1.000 | 1.001 | 1.001 | 1.000 | 0.554 | 0.535 | 1.000 | 0.961 | 0.960 | 1.000 | 1.059 | 1.073 |
| | Min. | 1.000 | 1.000 | 0.999 | 1.000 | 1.000 | 0.995 | 1.000 | 0.000 | 0.000 | 1.000 | 0.857 | 0.857 | 1.000 | 1.038 | 1.030 |
| | Max. | 1.000 | 1.000 | 1.000 | 1.000 | 1.167 | 1.167 | 1.000 | 4.000 | 4.000 | 1.000 | 1.064 | 1.064 | 1.000 | 1.111 | 1.111 |
| | Geo. Mean | 1.000 | 1.000 | 1.000 | 1.000 | 1.000 | 1.000 | 1.000 | 0.856 | 0.734 | 1.000 | 0.993 | 0.988 | 1.000 | 1.065 | 1.062 |

with the RL-S curve, the TL curve drops much faster, indicating the effectiveness of the proposed TL technique compared with training from scratch. We also observe that the #violation of the average TL and RL-S curves can go much higher than that of the RL curve between 0 to 20 K episodes. This is because the performance oscillates greatly at the beginning of the training iterations, several extremely poor points cause large average number of violations. With the training continuing, the performance gradually converges and becomes more stable.

In the previous section, we observe that the numbers of DRC violations for `ISPD18_test2/4/10` and `ISPD19_test2/4/5/6` are larger than Dr.CU's results. With our TL technique, `ISPD18_test4` and `ISPD19_test2` can outperform Dr.CU, while the results for `ISPD18_test2/10` and `ISPD19_test4/5/6` are still not as good as Dr.CU, especially that the results of `ISPD18_test10` and `ISPD19_test4/5/6` are far from expected. One possible reason lies in insufficient training, and the teacher network guides the student networks in the wrong direction. To verify that, we continue the training iterations of TL on these designs and report the numbers of DRC violations with the intermediate policies, as shown in Fig. 11. Each model is trained for 100 K–140 K episodes (around 100–140 h). Similar to that in Fig. 10, we only sample every 500, 1000, and 2000 episodes for each of the four designs mentioned above according to their sizes, respectively. We compare the TL curves with the results of Dr.CU and the RL algorithm, as well as the results of training from scratch ("RL-S"). Fig. 11 shows that in the first 3000 episodes (about 3 h), the model's performance improves slowly. When the training continues, the performance of the models keeps improving, even though with some turbulence. At around 80K–100K episodes, the performance of the TL algorithm approaches Dr.CU and eventually outperforms the latter with extra iterations. The best results in Fig. 11 can achieve approximately 4%, 17%, 6%, and 6% fewer DRC violations compared to Dr.CU, respectively. This experiment

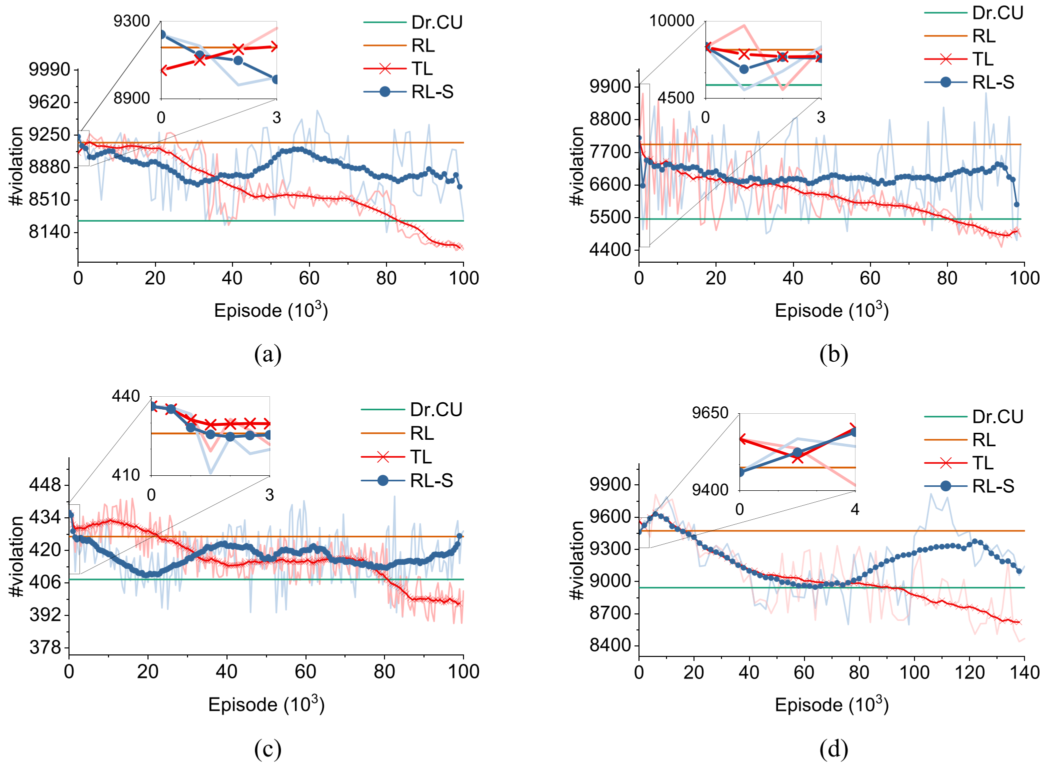


Fig. 11. Performance of policy distillation with additional training iterations on outlier designs, where "RL-S" represents the training results from scratch. The raw TL/RL-S results are shown in light red/blue, and the average TL/RL-S results are shown in the blue/green by taking an average of 25 data points around each point. We also zoom on the first ~3000 episodes to show the results at the beginning of the additional training iterations. (a) `ISPD18_test10`. (b) `ISPD19_test4`. (c) `ISPD19_test5`. (d) `ISPD19_test6`.

explains the reasons for the outliers in Table IV, and they can be resolved by continuing the policy distillation training until convergence. We also observe that the TL technique eventually leads to better convergence than training from scratch on these designs.

## VI. Conclusion

In this article, we proposed an asynchronous RL framework to search for high-quality net ordering strategies in detailed routing automatically. We proposed highly extensible agent models and mismatch penalty to enable efficient exploration of good policies. The experiments on ISPD 2018 and 2019 contest benchmarks demonstrate that our framework is able to learn an ordering policy that reduces the number of violations by 14 % on unseen benchmarks, compared with the state-of-the-art detailed router. We also proposed a TL algorithm to further improve the agent models' performance based on policy distillation. The models after TL can reduce the number of violations by 26 % on the testing designs. This study can enlighten techniques to automatically search for better routing solutions during design space exploration with extra computing resources or explore effective heuristics for routing.

Future work includes improving the agent network architecture to consider the correlation between multiple nets and expanding the state space to consider more features. We also plan to explore techniques [28] to handle the staleness between global and local agents in the asynchronous RL framework.

## References

[1] H.-Y. Chen and Y.-W. Chang, "Global and detailed routing," in *Electronic Design Automation*. Boston, MA, USA: Elsevier, 2009, pp. 687–749.

[2] J. Xu, X. Hong, T. Jing, Y. Cai, and J. Gu, "An efficient hierarchical timing-driven Steiner tree algorithm for global routing," *Integration*, vol. 35, no. 2, pp. 69–84, 2003.

[3] W.-H. Liu, W.-C. Kao, Y.-L. Li, and K.-Y. Chao, "NCTU-GR 2.0: Multithreaded collision-aware global routing with bounded-length maze routing," *IEEE Trans. Comput.-Aided Design Integr. Circuits Syst.*, vol. 32, no. 5, pp. 709–722, May 2013.

[4] S. Mantik, G. Posser, W.-K. Chow, Y. Ding, and W.-H. Liu, "ISPD 2018 initial detailed routing contest and benchmarks," in *Proc. Int. Symp. Phys. Design*, 2018, pp. 140–143.

[5] W.-H. Liu, S. Mantik, W.-K. Chow, Y. Ding, A. Farshidi, and G. Posser, "ISPD 2019 initial detailed routing contest and benchmark with advanced routing rules," in *Proc. Int. Symp. Phys. Design*, 2019, pp. 147–151.

[6] M. M. Ozdal and M. D. F. Wong, "Archer: A history-based global routing algorithm," *IEEE Trans. Comput.-Aided Design Integr. Circuits Syst.*, vol. 28, no. 4, pp. 528–540, Apr. 2009.

[7] T.-H. Wu, A. Davoodi, and J. T. Linderoth, "GRIP: Global routing via integer programming," *IEEE Trans. Comput.-Aided Design Integr. Circuits Syst.*, vol. 30, no. 1, pp. 72–84, Jan. 2011.

[8] M. M. Ozdal, "Detailed-routing algorithms for dense pin clusters in integrated circuits," *IEEE Trans. Comput.-Aided Design Integr. Circuits Syst.*, vol. 28, no. 3, pp. 340–349, Mar. 2009.

[9] T. Nieberg, "Gridless pin access in detailed routing," in *Proc. 48th ACM/EDAC/IEEE Design Autom. Conf. (DAC)*, San Diego, CA, USA, 2011, pp. 170–175.

[10] X. Xu, Y. Lin, V. Livramento, and D. Z. Pan, "Concurrent pin access optimization for unidirectional routing," in *Proc. 54th ACM/EDAC/IEEE Design Autom. Conf. (DAC)*, Austin, TX, USA, 2017, pp. 1–6.

[11] M. Ahrens *et al.*, "Detailed routing algorithms for advanced technology nodes," *IEEE Trans. Comput.-Aided Design Integr. Circuits Syst.*, vol. 34, no. 4, pp. 563–576, Apr. 2015.

[12] Q. Ma, H. Zhang, and M. D. F. Wong, "Triple patterning aware routing and its comparison with double patterning aware routing in 14nm technology," in *Proc. 49th Annu. Design Autom. Conf.*, San Francisco, CA, USA, 2012, pp. 591–596.

[13] Y.-H. Lin, B. Yu, D. Z. Pan, and Y.-L. Li, "TRIAD: A triple patterning lithography aware detailed router," in *Proc. Int. Conf. Comput.-Aided Design*, San Jose, CA, USA, 2012, pp. 123–129.

[14] Z. Liu, C. Liu, and E. F. Y. Young, "An effective triple patterning aware grid-based detailed routing approach," in *Proc. Design Autom. Test Eur. Conf. Exhibit. (DATE)*, Grenoble, France, 2015, pp. 1641–1646.

[15] A. B. Kahng, L. Wang, and B. Xu, "TritonRoute: An initial detailed router for advanced VLSI technologies," in *Proc. IEEE/ACM Int. Conf. Comput.-Aided Design (ICCAD)*, San Diego, CA, USA, 2018, pp. 1–8.

[16] G. Chen, C.-W. Pui, H. Li, and E. F. Y. Young, "Dr. CU: Detailed routing by sparse grid graph and minimum-area-captured path search," *IEEE Trans. Comput.-Aided Design Integr. Circuits Syst.*, vol. 39, no 9, pp. 1902–1915, Sep. 2020.

[17] H. Li, G. Chen, B. Jiang, J. Chen, and E. F. Y. Young, "Dr. CU 2.0: A scalable detailed routing framework with correct-by-construction design rule satisfaction," in *Proc. IEEE/ACM Int. Conf. Comput.-Aided Design (ICCAD)*, Westminster, CO, USA, Nov. 2019, pp. 1–7.

[18] S. M. M. Gonçalves, L. S. Rosa, and F. S. Marques, "DRAPS: A design rule aware path search algorithm for detailed routing," *IEEE Trans. Circuits Syst. II, Exp. Briefs*, vol. 67, no. 7, pp. 1239–1243, Jul. 2020.

[19] G. Liu, Z. Zhuang, W. Guo, and T.-C. Wang, "RDTA: An efficient routability-driven track assignment algorithm," in *Proc. Great Lakes Symp. VLSI*, 2019, pp. 315–318.

[20] F.-K. Sun, H. Chen, C.-Y. Chen, C.-H. Hsu, and Y.-W. Chang, "A multithreaded initial detailed routing algorithm considering global routing guides," in *Proc. IEEE/ACM Int. Conf. Comput.-Aided Design (ICCAD)*, San Diego, CA, USA, 2018, pp. 1–7.

[21] G. Chen, C.-W. Pui, H. Li, J. Chen, B. Jiang, and E. F. Y. Young, "Detailed routing by sparse grid graph and minimum-area-captured path search," in *Proc. 24th Asia South Pac. Design Autom. Conf.*, 2019, pp. 754–760.

[22] H. Liao *et al.*, "Attention routing: Track-assignment detailed routing using attention-based reinforcement learning," 2020. [Online]. Available: arXiv:2004.09473.

[23] X. Jia, Y. Cai, Q. Zhou, and B. Yu, "A multicommodity flow-based detailed router with efficient acceleration techniques," *IEEE Trans. Comput.-Aided Design Integr. Circuits Syst.*, vol. 37, no. 1, pp. 217–230, Jan. 2018.

[24] A. B. Kahng, L. Wang, and B. Xu, "TritonRoute: The open-source detailed router," *IEEE Trans. Comput.-Aided Design Integr. Circuits Syst.*, vol. 40, no. 3, pp. 547–559, Mar. 2021.

[25] V. Mnih *et al.*, "Asynchronous methods for deep reinforcement learning," Jun. 2016. [Online]. Available: arXiv:1602.01783.

[26] K. Lin, S. Wang, and J. Zhou, "Collaborative deep reinforcement learning," 2017. [Online]. Available: arXiv:1702.05796.

[27] T. Qu, Y. Lin, Z. Lu, Y. Su, and Y. Wei, "Asynchronous reinforcement learning framework for net order exploration in detailed routing," in *Proc. Design Autom. Test Eur. Conf. Exhibit. (DATE)*, Grenoble, France, Feb. 2021, pp. 1815–1820.

[28] I.-J. Liu, R. A. Yeh, and A. G. Schwing, "High-throughput synchronous deep RL," 2020. [Online]. Available: arXiv:2012.09849.

**Yibo Lin** (Member, IEEE) received the B.S. degree in microelectronics from Shanghai Jiaotong University, Shanghai, China, in 2013, and the Ph.D. degree from the Electrical and Computer Engineering Department, University of Texas at Austin, Austin, TX, USA, in 2018.

He is currently an Assistant Professor with the Computer Science Department associated with the Center for Energy-Efficient Computing and Applications, Peking University, Beijing, China. His research interests include physical design, machine learning applications, and GPU acceleration.

Dr. Lin has received four Best Paper Awards at premier venues (ISPD 2020, DAC 2019, VLSI Integration 2018, and SPIE 2016). He has also served in the Technical Program Committees of many major conferences, including ICCAD, ICCD, ISPD, and DAC.

**Tong Qu** received the B.S. degree in electronic science and technology from Tiangong University, Tianjin, China, in 2018, and the M.S. degree from the Department of Electronics and Communication Engineering, Institute of Microelectronics, Chinese Academy of Sciences, Beijing, China, in 2021.

His research interests include physical design and design for manufacturability.

**Zongqing Lu** received the B.S. and M.S. degrees from Southeast University, Nanjing, China, in 2005 and 2009, respectively, and the Ph.D. degree from Nanyang Technological University, Singapore, in 2014.

He is an Assistant Professor with the Department of Computer Science, Peking University, Beijing, China. Prior to joining Peking University in 2017, he worked as a Postdoctoral Researcher with the Department of Computer Science and Engineering, Pennsylvania State University, State College, PA, USA. His research interests include (multiagent) reinforcement learning and intelligent distributed systems.

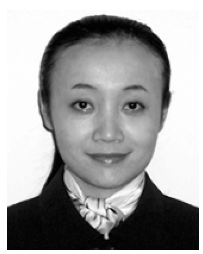

**Yajuan Su** received the B.S. and M.S. degrees in microelectronics from the University of Electronic Science and Technology of China, Chengdu, China, in 1995 and 1998, respectively, and the Ph.D. degree in microelectronics from Tsinghua University, Beijing, China, in 2005.

She is currently a Professor with the Institute of Microelectronics, Chinese Academy of Sciences, Beijing, and also with the Department of Computational Lithography, Guangdong Greater Bay Area Applied Research Institute of Integrated Circuit and Systems, Guangdong, China. Her research areas include design technology co-optimization and deep learning algorithms of IC design/manufacture flow.

**Yayi Wei** received the M.S. degree in electrics from the Institute of Electrics, Chinese Academy of Sciences, Beijing, China, in 1992, and the Ph.D. degree from the Max Planck Institute for Solid State Research/University Stuttgart, Stuttgart, Germany, in 1998.

He is currently a Professor with the Institute of Microelectronics, Chinese Academy of Sciences, and also with the Department of Computational Lithography, Guangdong Greater Bay Area Applied Research Institute of Integrated Circuit and Systems, Guangdong, China. His research interests include immersion lithography process and computational lithography, lithography materials, and equipment.